

Supporting Information

Rational Design of Covalent Triazine Frameworks Based on Pore Size and Heteroatomic toward High Performance Supercapacitors

Yunrui Zhang,^{a,‡} Boying Zhang,^{a,d,e,‡} Lifang Chen,^a Ting Wang,^{c,*} Mengyu

Di,^a Fei Jiang,^{b,*} Xiaoyang Xu,^a Shanlin Qiao^{a,d,*}

^a College of Chemistry and Pharmaceutical Engineering, Hebei

University of Science and Technology, Shijiazhuang 050018, China

^b College of Chemical and Environmental Engineering, Shanghai Institute
of Technology, Haiquan Road 100, Shanghai 201418, China.

^c CAS Key Laboratory of Bio-based Materials, Qingdao Institute of
Bioenergy and Bioprocess Technology, Chinese Academy of Sciences,
Qingdao 266101, China.

^d International Joint Laboratory of New Energy, Hebei University of
Science and Technology, Shijiazhuang 050018, People's Republic of
China

^e Department of Chemical Engineering, Faculty of Engineering and the
Built Environment, University of Johannesburg, Doornfontein 2028,
South Africa

‡ Both authors contribute equally to this work.

Content

Fig. S1. FT-IR spectra of CTF-1, DCE-CTF, BPY-CTF and DCP-CTF.

Fig. S2. (a) The Raman spectra and XRD patterns (b) of CTF-1, DCE-CTF, BPY-CTF and DCP-CTF.

Fig. S3. (a)–(d) The SEM images and (e)–(h) the TEM images of CTF-1, DCE-CTF, BPY-CTF and DCP-CTF.

Fig. S4. N₂ adsorption–desorption isotherms and the calculated pore parameters of CTF-1, DCE-CTF, BPY-CTF, and DCP-CTF.

Fig. S5. The XPS for CTF-1, DCE-CTF, BPY-CTF and DCP-CTF.

Fig. S6. Equivalent circuit of the impedance spectra.

Fig. S7. CV and GCD curves of CTF-1, DCE-CTF, and DCP-CTF at different scan rate.

Table S1. BET Surface areas of CTF-1, DCE-CTF, BPY-CTF and DCP-CTF.

Table S2. Nitrogen content of CTF-1, DCE-CTF, BPY-CTF and DCP-CTF from XPS.

Table S3. Peak areas of three kinds of N-configurations in CTFs, which are got from the deconvolution analysis results of N 1s.

Table S4. Summary of electrochemical performance of CTFs as electrode materials for supercapacitors.

Table S5. DFT specific surface areas and specific surface areas derived from micropores and mesopores of CTF-1, DCE-CTF, BPY-CTF and DCP-CTF.

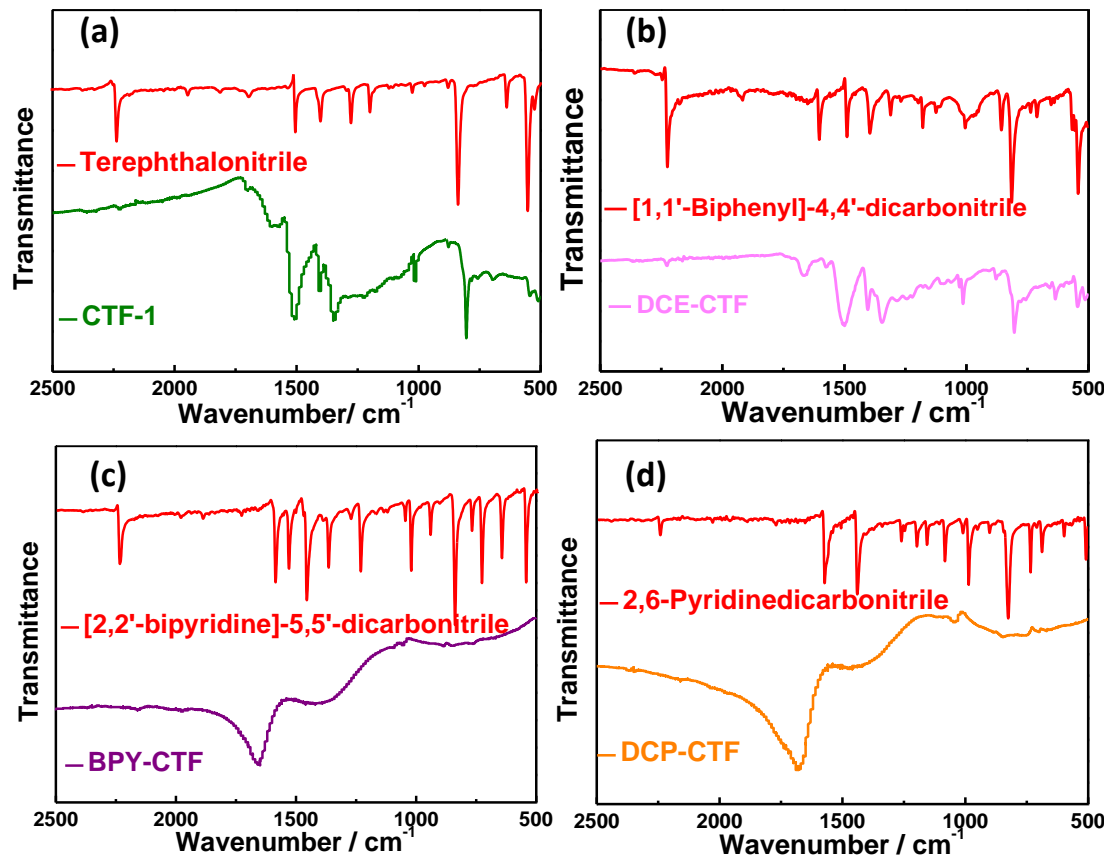


Fig. S1. FT-IR spectra of terephthalonitrile, [1,1'-biphenyl]-4,4'-dicarbonitrile, [2,2'-bipyridine]-5,5'-dicarbonitrile, pyridine-2,6-dicarbonitrile, CTF-1, DCE-CTF, BPY-CTF and DCP-CTF.

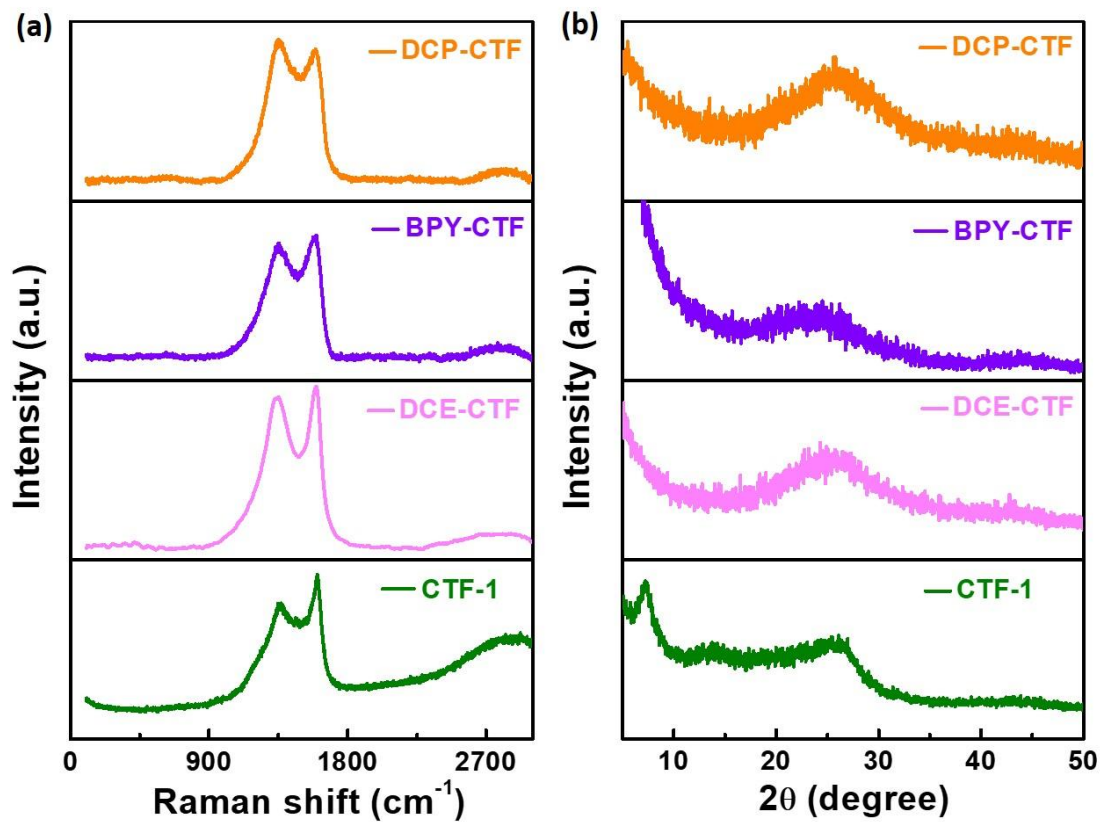


Fig. S2. (a) The Raman spectra and (b) XRD patterns of CTF-1, DCE-CTF, BPY-CTF and DCP-CTF.

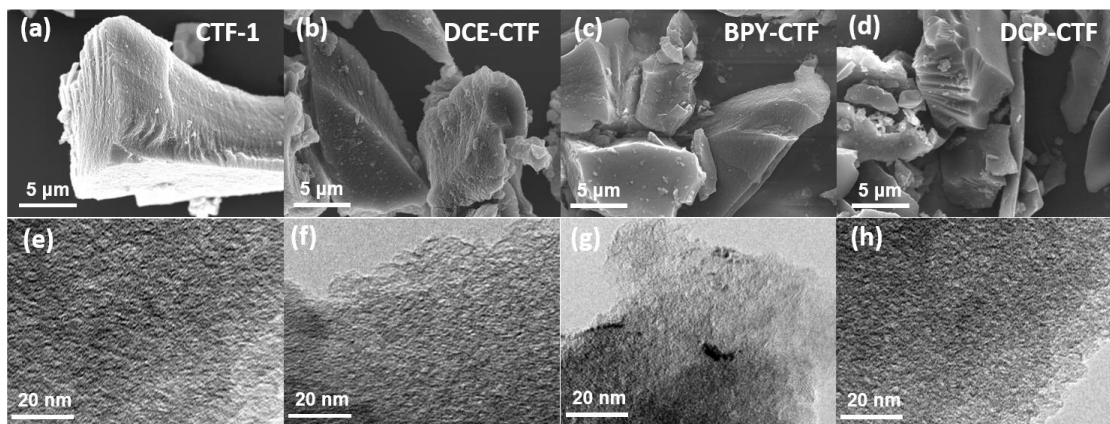
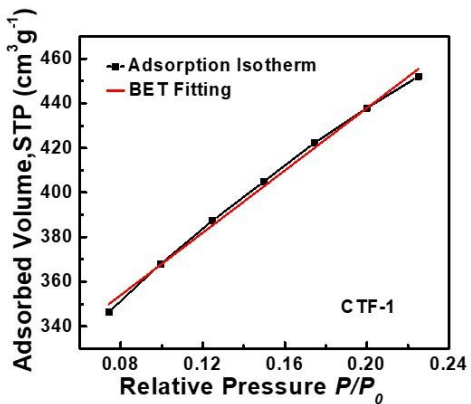
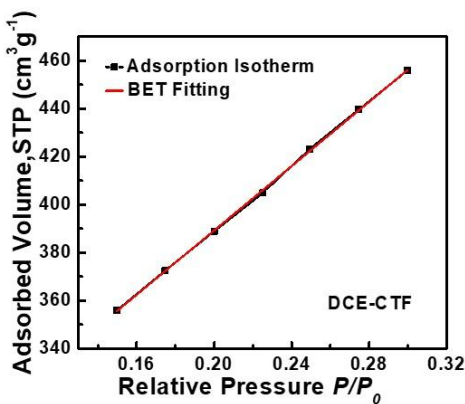


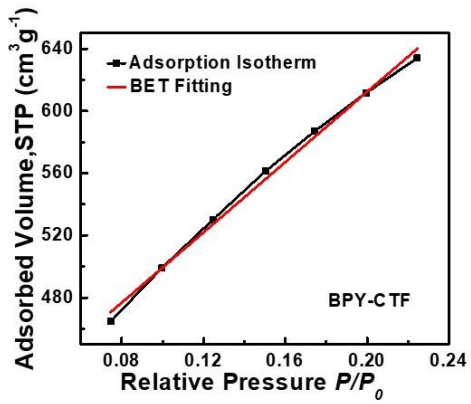
Fig. S3. (a)–(d) The SEM images and (e)–(h) the TEM images of CTF-1, DCE-CTF, BPY-CTF and DCP-CTF.



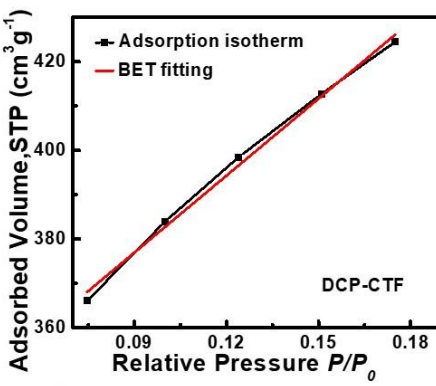
Slope = 2.170
 Intercept = 2.368e-02
 Correlation coefficient, r = 0.999945
 C constant= 92.619
 Surface Area = 1587.681 $\text{m}^2 \text{g}^{-1}$



Slope = 2.357
 Intercept = 4.265e-02
 Correlation coefficient, r = 0.999936
 C constant= 56.269
 Surface Area = 1451.199 $\text{m}^2 \text{g}^{-1}$



Slope = 1.501
 Intercept = 2.707e-02
 Correlation coefficient, r = 0.999947
 C constant= 56.470
 Surface Area = 2278.290 $\text{m}^2 \text{g}^{-1}$



Slope = 1.537
 Intercept = 2.463e-02
 Correlation coefficient, r = 0.999970
 C constant= 63.420
 Surface Area = 2229.773 $\text{m}^2 \text{g}^{-1}$

Fig. S4. N₂ adsorption–desorption isotherms and the calculated pore parameters of CTF-1, DEC-CTF, BPY-CTF, and DCP-CTF.

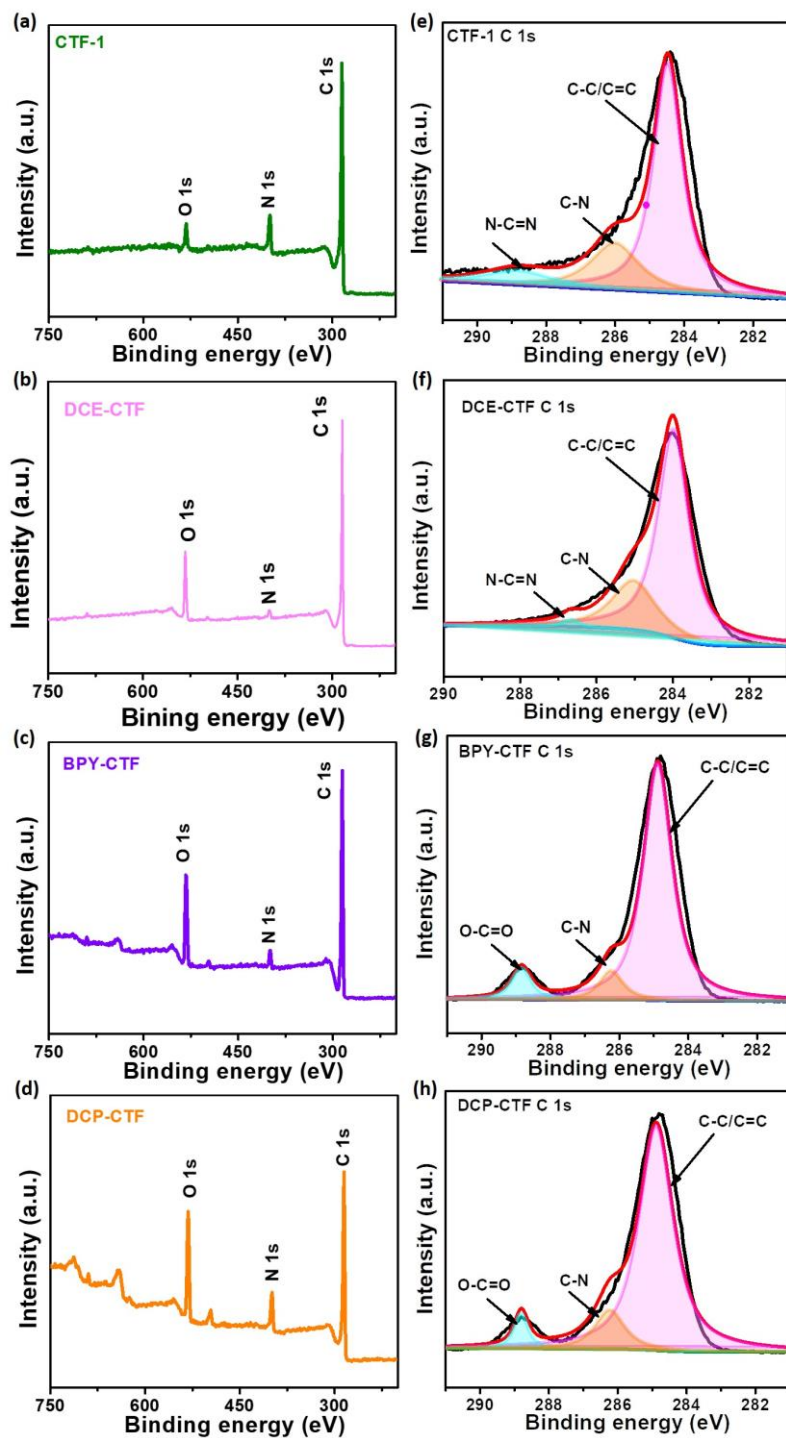


Fig. S5. The XPS for CTF-1, DCE-CTF BPY-CTF and DCP-CTF.

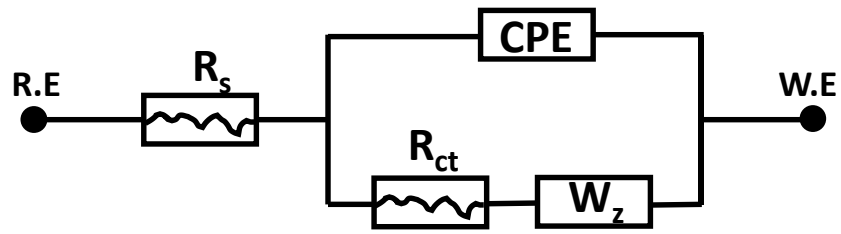


Fig. S6. Equivalent circuit of the impedance spectra.

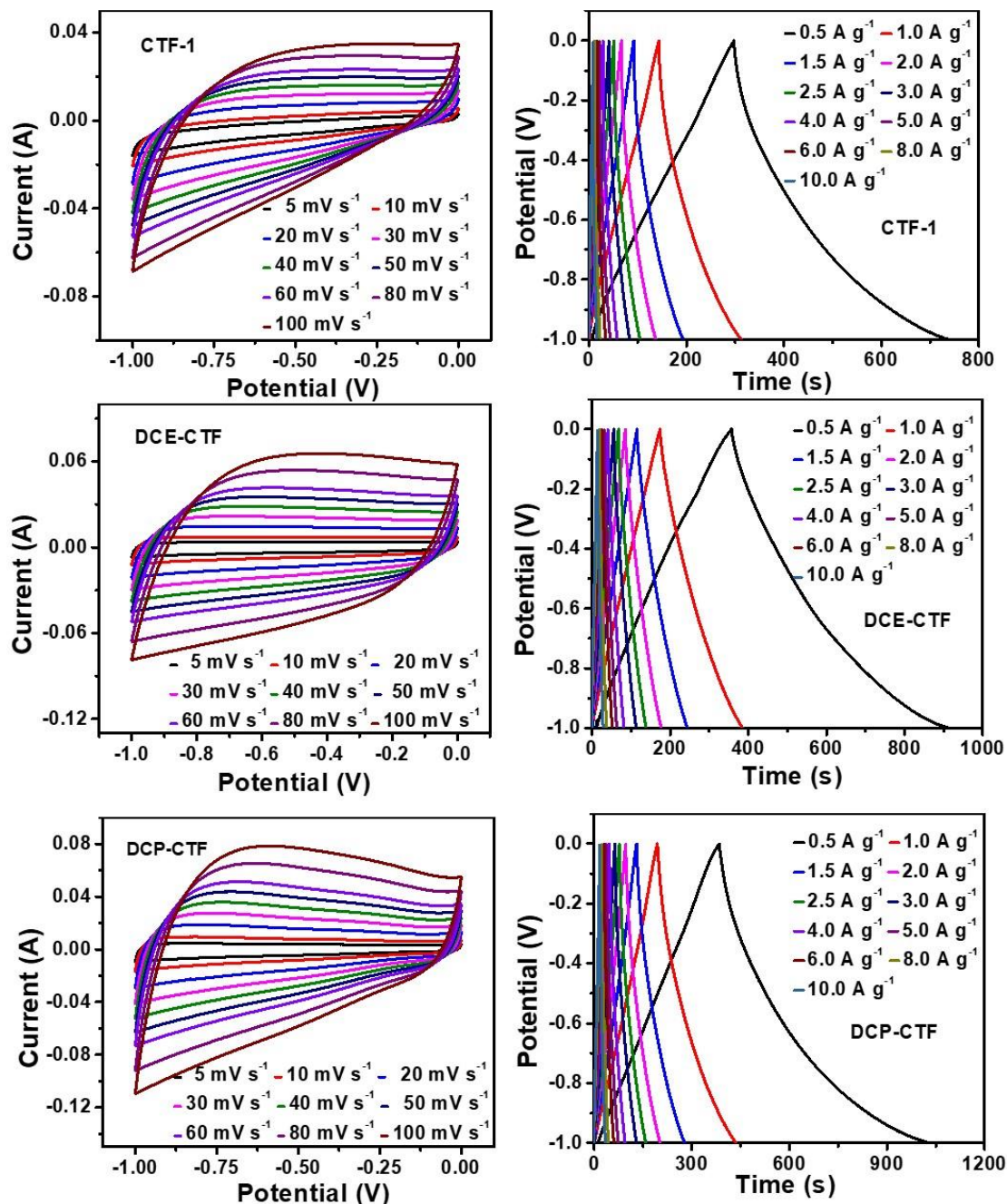


Fig. S7. CV cures and GCD cures of CTF-1, DCE-CTF, and DCP-CTF at different scan rate.

Table S1. BET Surface areas, micropores specific surface area, mesoporous specific surface area, and total pore volume of CTF-1, DCE-CTF, BPY-CTF and DCP-CTF.

Electrode materials	BET specific surface areas ($\text{m}^2 \text{ g}^{-1}$)	Micropores area ($\text{m}^2 \text{ g}^{-1}$)	Mesoporous area ($\text{m}^2 \text{ g}^{-1}$)	Total Pore Volume ($\text{cm}^3 \text{ g}^{-1}$)
CTF-1	1558	934	624	0.978
DCE-CTF	1451	0	1451	1.620
BPY-CTF	2278	990	1288	1.485
DCP-CTF	2229	844	1384	1.493

Table S2. Nitrogen contents of CTF-1, DCE-CTF, BPY-CTF and DCP-CTF from XPS.

Electrode materials	Nitrogen contents (%)
CTF-1	11.8
DCE-CTF	4.7
BPY-CTF	11.3
DCP-CTF	13.0

Table S3. Peak areas of three kinds of N-configurations in CTFs, which are got from the deconvolution analysis results of N 1s.

Electrode materials	N _{pyridinic}	N _{pyrrolic}	N _{quaternary}
CTF-1	6695	4030	3014
DCE-CTF	4224	5125	3812
BPY-CTF	11421	10393	10695
DCP-CTF	14546	8423	9933

$$\text{The ration of } N_x = \frac{N_x}{N_{\text{pyridinic}} + N_{\text{pyrrolic}} + N_{\text{quaternary}}}$$

Table S4. Summary of electrochemical performance of CTFs as electrode materials for supercapacitors.

Electrode materials	Electrolytes	Specific capacitance (F·g ⁻¹)	Ref
PDC-MA-COF	6 M KOH	335@1 A·g ⁻¹	S1
N-PC	6 M KOH	112@1 A·g ⁻¹	S2
TPT-DAHQ COF	1 M KOH	256@1 A·g ⁻¹	S3
TCNQ-CTF-800	1 M KOH	380@0.2 A·g ⁻¹	S4
TDFP-1	0.1 M H ₂ SO ₄	354@2.0 mV s ⁻¹	S5
p-CTF-600	1 M H ₂ SO ₄	340.1@0.2 A·g ⁻¹	S6
Car-CTFs	1 M KCl	545@5 mV s ⁻¹	S7
PTF-700	EMIMBF ₄	151.3@0.1 A·g ⁻¹	S8
G-PCs	6 M KOH	340@0.1 A·g ⁻¹	S9
FUM-700	6 M KOH	400@1 A·g ⁻¹	S10
LNU-18-800	6 M KOH	269@0.5 A·g ⁻¹	S11
AC-900	6 M KOH	278@1 A·g ⁻¹	S12
TPDA-1	1 M H ₂ SO ₄	469.4 F@2 mV s ⁻¹	S13
FCTF	1 M H ₂ SO ₄	379@1 A·g ⁻¹	S14
DCP-CTF-700	2.96 M ZnCl ₂	154@1 A·g ⁻¹	S15
BPY-CTF	1 M KOH	393.6@0.5 A g⁻¹	This work

Table S5. DFT specific surface areas and specific surface areas derived from micropores and mesopores of CTF-1, DCE-CTF, BPY-CTF and DCP-CTF.

Materials	DFT SSA	DFT SSA	Micropores SSA	Mesopores SSA
	$\text{m}^2 \text{ g}^{-1}$	$\text{m}^2 \text{ g}^{-1}$	$\text{m}^2 \text{ g}^{-1}$	$\text{m}^2 \text{ g}^{-1}$
CTF-1	1220	951	269	
DCE-CTF	1080	518	562	
BPY-CTF	1640	1210	430	
DCP-CTF	1660	1240	420	

References

- [S1] L. Li, F. Lu, R. Xue, B. Ma, Q. Li, N. Wu, H. Liu, W. Yao, H. Guo, W. Yang, Ultrastable Triazine-Based Covalent Organic Framework with an Interlayer Hydrogen Bonding for Supercapacitor Applications. *ACS Appl Mater Interfaces* 11 (29), **2019**, 26355–63. [DOI: 10.1021/acsami.9b06867](https://doi.org/10.1021/acsami.9b06867).
- [S2] S. Vargheese, M. Dinesh, K. V. Kavya, D. Pattappan, K. R. T. Rajendra, Y. Haldorai Triazine-Based 2D Covalent Organic Framework-Derived Nitrogen-Doped Porous Carbon for Supercapacitor Electrode. *Carbon Lett* **2020**. [DOI: 10.1007/s42823-020-00190-6](https://doi.org/10.1007/s42823-020-00190-6).
- [S3] AFM El-Mahdy, Y.-H. Hung, T. H. Mansoure, H.-H. Yu, T. Chen, S.-W. Kuo, A Hollow Microtubular Triazine- and Benzobisoxazole-Based Covalent Organic Framework Presenting Sponge-Like Shells that Functions as a High-Performance Supercapacitor. *Chem Asian J* 14 (9), **2019**, 1429–35. [DOI: 10.1002/asia.201900296](https://doi.org/10.1002/asia.201900296).
- [S4] Y. Li, S. Zheng, X. Liu, P. Li, L. Sun, R. Yang, S. Wang, Z.-S. Wu, X. Bao, W.-Q. Deng, Conductive Microporous Covalent Triazine-Based Framework for High-Performance Electrochemical Capacitive Energy Storage. *Angew Chem Int Ed* 57 (27), **2018**, 7992–7996, [DOI: 10.1002/anie.201711169](https://doi.org/10.1002/anie.201711169).
- [S5] P. Bhanja, K. Bhunia, S. K. Das, D. Pradhan, R. Kimura, Y. Hijikata, S. Irle, A. Bhaumik, A New Triazine-Based Covalentorganic Framework for High-Performance Capacitive Energy Storage. *Angew Chem Int Ed* 10 (5), **2017**, 921–929. [DOI: 10.1002/cssc.201601571](https://doi.org/10.1002/cssc.201601571).
- [S6] C. Wu, H. Zhang, M. Hu, G. Shan, J. Gao, J. Liu, X. Zhou, J. Yang, In Situ

Nitrogen-Doped Covalent Triazine-Based Multiporous Cross-Linking Framework for High-Performance Energy Storage. *Adv Electron Mater* 6 (7), **2020**, 2000253. [DOI: 10.1002/aelm.202000253.](https://doi.org/10.1002/aelm.202000253)

[S7] M. G. Mohamed, A. F. M. EL-Mahdy, M. M. M. Ahmed, S.-W. Kuo, Direct Synthesis of Microporous Bicarbazole-Based Covalent Triazine Frameworks for High-Performance Energy Storage and Carbon Dioxide Uptake. *ChemPlusChem* 84 (11), **2019**, 1767–1774, [DOI: 10.1002/cplu.201900635](https://doi.org/10.1002/cplu.201900635).

[S8] L. Hao, J. Ning, B. Luo, B. Wang, Y. Zhang, Z. Tang, J. Yang, A. Thomas, L. Zhi, Structural Evolution of 2D Microporous Covalent Triazine-Based Framework toward the Study of High-Performance Supercapacitors. *J Am Chem Soc* 137 (1), **2015**, 219–25. [DOI: 10.1021/ja508693y](https://doi.org/10.1021/ja508693y).

[S9] J. Zhu, X. Zhuang, J. Yang, X. Feng, S-i. Hirano, Graphene-Coupled Nitrogen-Enriched Porous Carbon Nanosheets for Energy Storage. *J Mater Chem A* 5 (32), **2017**, 16732–16739. [DOI: 10.1039/C7TA04752E](https://doi.org/10.1039/C7TA04752E).

[S10] D.-G. Wang, H. Wang, Y. Lin, G. Yu, M. Song, W. Zhong, G.-C. Kuang, Synthesis And Morphology Evolution of Ultrahigh Content Nitrogen-Doped, Micropore-Dominated Carbon Materials as High-Performance Supercapacitors. *Chemsuschem* 11 (22), **2018**, 3932–3940. [DOI: 10.1002/cssc.201801892](https://doi.org/10.1002/cssc.201801892).

[S11] Y. Zhao, N. Bu, H. Shao, Q. Zhang, B. Feng, Y. Xu, G. Zheng, Y. Yuan, Z. Yan, L. Xia, A Carbonized Porous Aromatic Framework to Achieve Customized Nitrogen Atoms for Enhanced Supercapacitor Performance. *New J Chem* 43 (46), **2019**, 18158–18164. [DOI: 10.1039/C9NJ04038B](https://doi.org/10.1039/C9NJ04038B).

- [S12] M. Kim, P. Puthiaraj, Y. Qian, Y. Kim, S. Jang, S. Hwang, E. Na, W.-S. Ahn, S. E. Shim, High Performance Carbon Supercapacitor Electrodes Derived from a Triazine-Based Covalent Organic Polymer with Regular Porosity. *Electrochim Acta* 284, **2018**, 98–107. [DOI: 10.1007/S0013468618315974](https://doi.org/10.1007/S0013468618315974).
- [S13] P. Bhanja, S. K. Das, K. Bhunia, D. Pradhan, T. Hayashi, Y. Hijikata, S. Irle, A. Bhaumik, A New Porous Polymer for Highly Efficient Capacitive Energy Storage. *ACS Sustain Chem Eng* 6 (1), **2018**, 202–209. [DOI: 10.1021/acssuschemeng.7b02234](https://doi.org/10.1021/acssuschemeng.7b02234).
- [S14] Y. Gao, C. Zhi, P. Cui, K. Zhang, L.-P. Lv, Y. Wang, Halogen-Functionalized Triazine-Based Organic Frameworks towards High Performance Supercapacitors. *Chem Eng J* 400, **2020**, 125967. [DOI: S1385894720320957](https://doi.org/10.1385894720320957).
- [S15] E. Troschke, D. Leistenschneider, T. Rensch, S. Grätz, J. Maschita, S. Ehrling, B. Klemmed, B. V. Lotsch, A. Eychmüller, L. Borchardt, S. Kaskel, In Situ Generation of Electrolyte inside Pyridine-Based Covalent Triazine Frameworks for Direct Supercapacitor Integration. *Chemsuschem* 13 (12), **2020**, 3192–3198. [DOI: 10.1002/cssc.202000518](https://doi.org/10.1002/cssc.202000518).